Metal Ammonia solutions

Mitchell Watts

June 2016

1 Introduction

1.1 History

The earliest observation of the blue and bronze colours associated with metal-ammonia solutions can be attributed to Sir Humphrey Davy [REF]. In 1807 Davy, in the pursuit of proof that potassium was an element, reacted grains of potassium with dry, gaseous ammonia, he noted the 'fine blue colour' observed upon this dissolution.

In 1864, W. Weyl made independent observations of this type, however he mistakenly called these solutions 'metal ammoniums'[REF]. It wasn't until C. Seely in 1871 [REF] that it was discovered that this was a 'non chemical' solvent action of ammonia on the alkali metals - noted by the recovery of the metal upon boiling of NH_3.

It was Kraus that first suggested that in dilute solutions the electron is surrounded by an 'envelope of solvent'[REF]. This idea will be discussed and built upon later.

Much controversy over the nature of these solutions has existed over the 200 years since its first discovery, and debate still exists today regarding some interesting aspects of these and related species.

1.2 Ammonia as a solvent

It is useful to note several similarities and differences between ammonia and water as a solvent[REF]:

- Water has a higher low-frequency permittivity (80 versus 22 at $20\,\mathrm{deg}\,C$)
- Hydrogen boding is much more important in solvent-solvent interactions in H_2O than in NH_3
- NH_3 is more stable against dissociation in the liquid than water is (0.1 ppm in H_2O v 10^{-10}ppm in NH_3) - note this means ammonia is much more stable for solvating electrons than water

1.2.1 Electronic properties

Alkali metals have the following ionization energies (in the gas phase)[REF]:

- 5.39eV for Li
- 5.14eV for N
- 4.34eV for K

For NH_3, we see that there are 3 empty molecular orbitals, equivalent to anti bonding N-H orbitals[REF]. The ionization energy of ammonia is 10.86eV, but the two lowest energy transitions between molecular orbits are at 6.5eV and 8.0eV. Also note that ammonia doesn't have a positive electron affinity and so doesn't bind an excess electron.

1.3 Metals, concentrations and temperature regimes

Metal-ammonia solutions can be prepared using the following metals[REF]:

- Li
- Na
- K
- Rb
- Cs
- Ca
- Sr
- Ba
- Yb
- Eu
- Cations such as tetra-alkyl-ammonium can also be used
- Electrons can also be directly injected into ammonia via pulsed radiolysis

For all solutions the freezing point of ammonia is suppressed when metals are dissolved - this is true at all concentrations, which can be as low as 89K, versus the 195.4K melting point of pure ammonia[REF].

Many metals have a 'miscibility gap' on their phase diagrams (note this isn't seen for Cs). This is a region where there is a phase separation of two concentrations of solution, which are immiscible with each other. The reasons for these gaps are discussed later.

1.4 Uses

Metal-ammonia solutions are known to be extremely reducing, the solvated electron (discussed later) reacts with oxygen to form a super-oxide radical, which is a potent oxidant[REF]. It can also form hydroxyl radicals when mixed with nitrous oxide[REF]. Current uses include the Birch reduction and the Bouveault-Blanc reduction[REF], which are used to attach hydrogen to aromatic compounds and to reduce an ether to primary alcohols (note this uses ethanol as the solvent not ammonia) respectively.

A recent use of these solutions are in the field of nano-physics, where it has been shown that they can successfully intercalate layered materials (also to reduce carbon nano-tubes) to form salts as an intermediary step in liquid phase exfoliation[REF].

2 Preparation and Phase Diagrams

2.1 Dissolution and dissociation

Upon addition of an alkali metal (or any of the species noted in section 1.3), the electron is liberated from the metal in the following manner[REF]:

$$M \rightarrow M^+ + e^- \tag{2.1}$$

This equation is at the heart of these solutions. A detailed list of the species present in these solutions will be given below, however there are essentially two regimes for metal-ammonia solutions; 1) a dilute phase where the electron is solvated by ammonia molecules 2) a concentrated phase where the electron is dissociated from the metal completely, and the solutions acts like a metal- for reasons discussed later. We will explore which species are present and the properties of these species in this section.

2.2 An outline of the many species

Metal-ammonia solutions are extremely complex with many molecular species existing across a huge range of concentrations. Figure 2 shows a simplified view of these species, with an indication of the regimes they exist within. Reasons for the transition between these molecular species as more metal is added will be discussed in later sections.

The species shown in figure 2 are outlined below, and some are shown schematically in figure 2. Note only Li solutions are considered here, although similar species are to be expected for other metals in the same group (excluding Cs?).

The following notation is used:

- @ is used to denote an electron with wave-function delocalised over a group of ammonias (i.e. solvated)
- '$\cdot$' represents association of species
- $\leftrightarrow$ is for continuum of states

Also get coupled radicals (CR) which are a single unpaired electron in the species.

The molecular characters are:

- S=0
  - $(NH_3)_n$, single ammonia or a cluster of ammonia molecules
  - $Li(NH_3)_4^+$ this can also be solvated via hydrogen bonding to more ammonia molecules
- S= $\frac{1}{2}$
  - $Li(NH_3)_4$ (q=0), the monomer
  - $e^-@(Nh_3)_n$ (q=-1), the solvated electron

Figure 1: A simplified view of the many species present in metal-ammonia solutions across a wide range of metal concentrations (REF)

  - $[Li(NH_3)_4 \cdot e^-@(Nh_3)_n]$ (q=0), via $Li(NH_3)_4$ associating with ammonia

- Coupled radicals form via e.g. $Li(NH_3)_4$ units aggregating to form S=0,1,2 etc... forming:
  - $[Li(NH_3)_4]_r$
  - $[Li(NH_3)_4^+ \cdot e^-@(NH_3)_n]_r$ (q=0)
  - $[Li(NH_3)_4 \cdot e^-@(NH_3)_n]$ (q=-1)
  - $2e^-@(Nh_3)_n$ (q=-2)
  - $[2e^-@(Nh_3)_n]_r$ (q=-2)

2.3 Phase diagrams

The phase diagrams for Li, K and Cs-ammonia solutions are included below. Note the differences in the miscibility gaps in each solution. Similar molecu-

Figure 2: A schematic view of the diamagnetic and paramagnetic species present in metal ammonia solutions (REF)

lar compounds are expected to exist in each regime as for Li. Note also the difference in the eutectic point, and the difference in MPM for concentration regimes.

Figure 3: The phase diagram for $Li - NH_3$ solutions (REF)

Figure 4: The phase diagram for $Ca - NH_3$ solutions (REF)

2.4 Decomposition

Metal-ammonia solutions are metastable, and so it is expected that decomposition will continually occur within these solutions. There are several factors which can affect the rate of decomposition:

Figure 5: The phase diagram for $Cs - NH_3$ solutions (REF)

- Impurities
- Electron scavenging
- Temperature

The decomposition reaction is as follows[REF]:

$$Na^+_{(s)} + e^-_{(s)} + NH_3 \rightarrow NaNH_{2(s)} + \frac{1}{2}H_{2(s)} \tag{2.2}$$

The rate of this reaction increases with temperature, and so keeping these solutions cool is imperative.

Impurities only act to increase the rate of this reaction, as they act as catalysts, it is therefore important that all materials involved in the production and use of these solutions are thoroughly cleaned. For ammonia this can be achieved by dissolving ammonia onto mechanically cleaved metal, and then, after several hours, cryo-pumping the ammonia back into a lecture bottle. The ammonia, when frozen, can then be pumped on to remove any hydrogen which will still be gaseous at liquid nitrogen temperatures. This produces amides which can be washed away. This method can also be used to clean glassware. Note glassware can hold 'electron scavenging sites' due to metal atoms, water or radicals which also catalyse the reaction shown in equation 2.2 [REF].

It is important to avoid decomposition when studying or using these solutions, as this will skew the concentration measured. In fact, it is suggested by Thompson that the concentration must necessarily be in error if it is determined by input metal and ammonia moles, however this error can be reduced with good practice [REF]. There is also the issue of gas evolution, which can be potentially explosive if appreciable decomposition occurs in a sealed container.

3 Metallic/Saturated Regime

3.1 Introduction

Figure 6 shows the variation of conductivity, σ, with molar percent metal (MPM) for $Na - NH_3$ solutions. A rapid increase in conductivity is seen for high concentrations with the saturated solution having a conductivity of 15,000 $\Omega^{-1}cm^{-1}$, higher than that of liquid mercury[REF]. In this discussion we will consider 8MPM as the onset of metallic behaviour.

The main species considered in this section are:

- $[Li(NH_3)_4^+ \cdot e^-@(NH_3)_n]_r$
- $2e^-@(NH_3)_n$
- $[Li(NH_3)_4]_r$
- $[Li(NH_3)_4 \cdot e^-@(NH_3)_n]$

Figure 6: The variation of σ with MPM for $Na - NH_3$ (REF)

3.2 The solvation shell

Neutron diffraction data puts 4 ammonia molecules in the first solvation shell, which is the simplest $S = \frac{1}{2}$ system, called the monomer[REF]. $Li(NH_3)_4^+$ is the most dominate ionic species in these solutions[REF]. DFT calculations confirm this is the most stable configuration, and adding a 5th molecule is not stable, but is loosely associated with molecule[REF].

It is suggested by DFT calculations that aggregation of the $Li(NH_3)_4$ complexes may be what causes the transition to the metallic state. It is thought that this allows solvated electrons to tunnel more easily between solvation shells, thus allowing metallization[REF].

The electron in these species is thought to reside between the N and H and tunnel between species[REF]. Edwards describes this as being due to $H \leftrightsquigarrow H$ bonding, a type of bonding between hydrogens due to an overlap of molecular orbitals.

3.3 Properties of the metallic liquids

3.3.1 Electrical conductivity

The electrical conductivity is often used to experimentally determine the concentration of the solution being studied. This can give a smaller uncertainty than that found by determining concentration from the starting products (note decomposition at electrodes does also have an uncertainty)[REF]. Techniques to measure the conductivity vary from four point probe DC, to techniques depending on Eddy currents.

Electrical conductivity is found to increase as a function of T, except for the most concentrated Li or Cs solutions, however an application of pressure reduces the conductivity in a linear fashion[REF].

3.3.2 Hall effect

The carrier density for more than 8MPM is equal to density of metal valence electrons and is independent of temperature, except for the effect of varying the density of the solution. This is as expected for a liquid metal.

The Hall mobility:

$$\mu_H = R_H \sigma \tag{3.1}$$

shows a strong concentration and temperature dependence[REF].

3.3.3 Density and viscosity

Density is a decreasing function of concentration, for lithium this approaches a density smaller than any other fluid (except the cryogenic liquids)[REF]. It is an approximately linear function of metal concentration[REF].

Viscosity is a decreasing function of temperature[REF].

3.3.4 Optical data

Optical data has been collected by measuring the normal reflectance relative to mercury, or by ellipsometric techniques (measuring the parallel and perpendicular reflected amplitudes) to measure the real and imaginary parts of the dielectric constant as a function of concentration (note the imaginary part is concentration independent).

Drude theory [REF] assumes that the electrons in a metal are not bound to any nucleus and act independently of the nuclei, only colliding occasionally with them. This gives a rough agreement with the optical data for these systems (i.e. plasma frequency, skin depth etc.)[REF].

The energy loss function can be found from the imaginary part of the permittivity, the peak of which is related to the plasma frequency[REF]:

$$\epsilon = \epsilon_1 - \epsilon_2 = 1 + \frac{ne^2}{m(\omega^2 + \frac{i\omega}{\tau_{opt}})^{-1}} \tag{3.2}$$

$$e.l.f. = Im(\frac{1}{\epsilon}) = \frac{\epsilon^2}{\epsilon_1^2 + \epsilon_2^2} \tag{3.3}$$

where n is the carrier density, ω is the photon frequency, ω_1, ω_2 are the real and imaginary dielectric constants respectively and τ_{opt} is the electron relaxation time..

The carrier concentrations determined from Hall data and optical relaxation times are similar, although DC measurements give much larger electron relaxation times than those measured from optical data[REF]. The mean free paths and transport coefficients are within limits suggested by Allgaier for class A or B metals[REF]. Therefore electrons will freely propagate in the metallic phase rather than hop between sites.

3.3.5 Magnetic susceptibility and NMR

The static susceptibility is found to be weakly temperature dependent. Liquid ammonia is diamagnetic, and the addition of metal makes it less diamagnetic.

The Knight shift (i.e. shift in NMR spectrum due to electrons near the atom being probed), increases with temperature and concentration. The Knight shift is the same at equal concentrations for both Na and Cs[REF].

3.4 Models and explanations

Here a comparison is made with liquid metals, using the Drude model and Ziman theory. Some theory is presented, and deductions from available data are made based on this theory.

3.4.1 Ziman (NFE) theory

This sections describes the use of nearly free electron theory (NFE) to describe liquid metals[REF]. There are two fundamental assumptions in this theory:

- The Fermi is surface is spherical
- The density of states per unit energy, N(E), is appropriate to that for a free electron gas:

$$N(E) = \frac{V}{2\pi}(\frac{2m}{\hbar^2})^{\frac{3}{4}} E^{\frac{1}{2}} \tag{3.4}$$

The mean free path, Λ, is related to the conductivity by[REF]:

$$\sigma = \frac{e^2 \Lambda \nu}{12\pi^3 \hbar} \tag{3.5}$$

Where ν is the area of the Fermi surface.
The relaxation time is given by $\frac{\Lambda}{\hbar k_F}$, which is also equal to [REF]:

$$\tau^{-1} = \int dv(1 - cos\theta) P_{kk'} \tag{3.6}$$

The probability per unit time of scattering of an electron can be given by Fermi's golden rule:

$$P_{kk'} = \frac{2\pi}{\hbar}\Big|\langle K'|W|K\rangle\Big|^2 N(E) \tag{3.7}$$

We can separate Fermi's golden rule into a structure dependent and independent part (letting k=K-K')[REF]:

$$\Big|\langle K'|W|K\rangle\Big|^2 = \frac{1}{V^2}|U(k)|^2|\sum exp(ik\cdot r_i)|^2 \tag{3.8}$$

U(k) is the form factor, which can be given by[REF]:

$$U(k) = \int exp(ik\cdot r)U(r)d^3r \tag{3.9}$$

The sum over ions in eq 3.8 can be related to the structure factor, a(k), by[REF]:

$$a(k) = \frac{1}{N}|\sum exp(ik\cdot r_i)|^2 \tag{3.10}$$

We therefore see that we can get an equation for the resistivity as[REF]:

$$\rho = \frac{4k_F m^2}{e^2\hbar^3}\frac{n_s}{n_e}\int_0^1 y^3|u(2k_F y)|^2 a(2k_F y)dy \tag{3.11}$$

where n_s, n_e are the number density of ions and electrons respectively, and $y = \frac{k}{2k_F}$.

Electron-electron interactions are included via the dielectric function, via the Hartree-Fock function[REF]:

$$\epsilon(k) = 1 + \frac{me^2}{\pi k_F\hbar^2 y^2}[\frac{1-y^2}{4y}ln|\frac{1+y}{1-y}| + \frac{1}{2}] \tag{3.12}$$

Free electron theory can also give the isothermal compressibility[REF]:

$$K_T = \frac{a(0)}{(nk_BT)} \tag{3.13}$$

3.4.2 Theory as applied to metal-ammonia systems

A sum rule exists for the relation of the optical energy loss function to the carrier density[REF]:

$$n = \frac{\epsilon_\infty m*}{2\pi^2 e^2}\int_0^\infty Im[\epsilon^{-1}(\omega)]\omega d\omega \tag{3.14}$$

This sum rule is independent of Drude theory, and is valid in the absence of inter-band transitions.

Experimental diffusion experiments suggest that the ions in these solutions are not moving, and the smaller ions are impeded in motion. This is because

self diffusion limits for both Li and H are practically equal regardless of concentration.

The Stokes-Einstein relation[REF]:

$$D = \frac{k_B T}{6\pi\eta r} \tag{3.15}$$

can be used to calculate radii for $Li(NH_3)_4^+$ and $Na(NH_3)_4^+$ complexes. These are found to be roughly equal, and approximately twice as large as the free ammonia radius, suggesting that the metal ion is solvated by ammonia[REF]. This model can be used to calculate physical properties using Ziman theory, discussed below.

3.4.3 The structure factor

The structure factor describes the interaction between the solvated ions and the ammonia molecules. This can allow us to the calculate a(k) which leads to a calculation of σ (together with U(k) discussed later).

The structure factor can be calculated by assuming that the free ammonia molecules and the solvated ions interact as hard spheres[REF]. We therefore can measure the isothermal compressibility at k=0 to get the ratio between the radius' of these hard spheres. In saturated regime there are no free ammonia molecules, and so the radius of the cavity can be found. Typically for $Li - NH_3$ systems this was found to be near 3Å.

However there is a problem due to the density, the metal can be described as being solvated, however the volume of the solution greatly exceeds that of the constituents, which gives rise to the idea of the solvated electron. If this is presumed to exist in a bubble near 1.7Åradius, then the calculated density matches the data[REF].

3.4.4 The form factor

The other factor in the resistivity is the form factor, U(k). Using random dipole potentials in the first Born approximation can lead us to a calculation of U(k)[REF]. Electron screening is such to reduce the tenancy of the dipoles to align, so that angular orientations are independent of spatial configurations. The dipole-dipole interaction terms then become structure and k independent. Therefore only the ion-ion interactions remain, these must be adjusted for the bound NH_3 dipole compared to the free dipole moment, due to polarisation produced by the field of the ion. We then get:

$$\rho \propto N_d \int_0^1 U_d^2(y) y^3 dy + N_i \int_0^1 U_{si}^2(y) a_{ii}(y) y^3 dy \tag{3.16}$$

Where U_d is the dipole point potential, N_d and N_i are the densities of free dipoles and solvated ions. U_{si} is the solvated ion potential, which includes the

coulomb field of the ion together with the dipole fields of the solvated NH_3 molecules.

The conductivity can then be calculated and U_A adjusted to fit the data. This gives U_A=0.4 in units of $\frac{2}{3}E_F$, in agreement with data throughout the metallic region at 240K.

3.4.5 Summary of model

The calculations find increasing order of solutions and decreasing NH_3 gives an increase in conductivity. Above 8MPM we therefore describe these systems as a binary mixture of solvated metal ions and solvent molecules, permeated by a free electron gas. Electronic measurements match this theory, however optical and magnetic data does not.

3.4.6 Optical data deductions

Simple metals have negligible core polarization contribution to their relative permittivity, however metal-ammonia solutions have a background permittivity due to NH_3. Metal-ammonia solutions therefore have ϵ_∞, which is approximately twice the vacuum value[REF]. So the plasma frequency and e.l.f. both shift down. ϵ_∞ can be estimated using the value for NH_3 of 1.9[REF]:

$$\epsilon = 1.9\alpha + (1 - \alpha) \tag{3.17}$$

Where α is the volume fraction of metal-ammonia solution.

Then the sum rule can be used, along with the plasma frequency[REF]:

$$n = \frac{\epsilon_\infty m^*}{2\pi^2 e^2} \int_0^\infty Im[\epsilon^{-1}(\omega)]\omega d\omega \tag{3.18}$$

$$\omega_p^2 = \frac{4\pi n e^2}{m^* \epsilon_\infty} \tag{3.19}$$

Note: plasma frequency can be derived as follows[REF]:

The response of an electron acting as a harmonic oscillator can be described as:

$$m\frac{d^2x}{dt^2} = -eE \tag{3.20}$$

If x and E have time dependence of the form $e^{-i\omega t}$, then:

$$-\omega^2 mx = -eE, x = \frac{eE}{m\omega^2} \tag{3.21}$$

The polarization, P, of an electron can be found from the dipole moment per unit volume:

$$P = np = -nex = \frac{-ne^2}{m\omega^2}E \tag{3.22}$$

The dielectric function at ω is defined as:

$$\epsilon(\omega) = \frac{D(\omega)}{E(\omega)} = \frac{E(\omega) + 4\pi P(\omega)}{E(\omega)} \tag{3.23}$$

Therefore:

$$\epsilon(\omega) = 1 - \omega_p^2 \tag{3.24}$$

where:

$$\omega_p^2 = \frac{ne^2}{\epsilon_0 m} \tag{3.25}$$

The free carrier density can be estimated by using ϵ^{-1} and compared to those measured via the Hall effect, but these don't match. This may be due to the sum rule assuming excess carriers due to excitation of core electrons, which doesn't happen below 4eV for metal ammonia solutions. The value also lies near the free electron value, so altering m* from that of an electron also improves agreement with data[REF].

By using the e.l.f. we can get the positions and half-width peak, which is placed (by Drude theory) at[REF]:

$$\omega_1 = [\omega_p^2 - (4\tau^2)^{-1}]^{\frac{1}{2}} \tag{3.26}$$

and the half-width is τ^{-1}. The peak is in the visible for the e.l.f., and this influences reflectivity, as this gives ϵ as negative below this point (plasma frequency) meaning that all light is reflected below this frequency of light (due to negative refractive index). Together with the usual band theory explanation of the appearance of metals, we see that this explains the golden colour of these solutions[REF].

4 Electrolytic regime

4.1 Introduction

This section will first focus on the regime from infinite dilution up to 1MPM, and then the intermediate regime from 1MPM up to metallization. This regime is called the electrolytic regime as many properties can be likened to those of salts dissolved in solvents e.g. the conductivity. Some properties can be likened to electrolytic solutions for low concentrations, however this theory is not presented here.

The dominant species in this regime is ammonia molecules hydrogen bonded together[REF]. As metal is added these ammonia molecules start to solvate the metal ions. We see that electron cavities appear, and at greater concentrations the electron and ion associate.

4.2 Properties of the electrolytic regime

The properties of these systems vary very little with changing solute. Here we explore the measured properties and how they vary with changing parameters.

4.2.1 Electrical properties

Conductivity is an increasing function of temperature and a decreasing function of pressure. Measurements on the transference, i.e. the fraction of each component which contributes to mobilities can be performed to indicate which species are responsible for mobilities. These are given by[REF]:

$$t_{\pm} = \frac{\mu_{\pm}}{\mu_{+} + \mu_{-}} \tag{4.1}$$

the ratio $\frac{t_-}{t_+}$ is found to be approximately 7, this means that the negative components contribute most to the mobility.

4.2.2 Optical data

Broad symmetric absorption lines are seen near 0.88eV for these solutions, with a long high energy tail, this is responsible for the blue colour of these solutions (see figure 7)[REF]. The absorption edge near the UV at 5eV is also enhanced and shifted to a lower energy (compared to in pure ammonia), and the molecular vibration spectrum of ammonia is also shifted.

The blue colour is seen to be independent of solute, and is thought to be caused by the solvated electron[REF]. This suggests that the trapped electron is completely remote and independent from the ionic potential.

4.2.3 Magnetic data

Magnetic susceptibility: The pure solvent is diamagnetic, the use of Weidemann's rule to get the atomic susceptibility can be used with limiting success. This gives the number density of valence electrons far above that found from data.

ESR: The Mott g factor is found from line shapes and widths at saturation[REF]. This is a measure of the magnetic moment of an electron, which is affected by its environment. This is found to be close to a free electron, independent of concentration and frequency.

NMR: The Knight shift describes a shift in the lines wrt pure ammonia, the metal nitrates or iodides[REF]. This is due to the different electron wavefunction near the atom. The Knight shift increases with T, and its measurement can give the electronic wave-function at the nucleus if the susceptibility is known.

$$K(N_i) = \frac{-8\pi}{3N_0}\chi\Big|\psi(N_i)\Big|^2 \tag{4.2}$$

The Knight shift suggests an Overhauser enhancement, which infers contact between an unpaired electron and a proton, adding to the idea of a solvated electron[REF]. There is also a strong electron-nitrogen interaction, and a weak cation-electron interaction, suggesting that the electron doesn't 'see' the metal ion in this concentration regime.

Figure 7: The absorption spectra of dilute metal-ammonia solutions

4.2.4 Physical properties

The density of these systems is lower than that observed for pure ammonia, and exceeds that of the constituents, this again is thought to be due to the solvated electron[REF].

The vapour pressure for these solutions is $\frac{1}{3}$ to $\frac{1}{5}$ that of pure ammonia[REF].

The viscosities are much lower than ammonia, and decreases linearly above 1MPM. The surface tension is measured by maximum bubble pressure, this is found to be much higher than ammonia, and increases significantly above 4MPM[REF].

4.3 Models and explanations

4.3.1 The solvated electron

The solvated electron is proposed as a model to fit several ideas in these solutions.

The following is a list of evidence for the existence of the solvated electron (in addition to DFT calculations)[REF]:

- Low, but non-zero, conductance
- The independence of the optical absorption upon solute
- The presence of unpaired electron spins
- The smallness of the solute Knight shift
- Large size of excess volume (a theoretical volume proposed in electrolyte theory to account for non-ideal behaviour of dissolved salts)
- Variation of viscosity with concentration
- Correlation of H and N Knight shifts
- Relaxation of electron spins by N interaction.

The steps for the solvation of an electron are shown in figure 8.

Note that the final step in the solvation of the electron is thermal agitation, whereby hydrogen bonding and dipole-dipole repulsion causes the cavity to expand to minimise the so called Bjerrum defects (caused by hydrogen bonds with one too many or too little hydrogens present)[REF].

A popular model for the solvated electron is that of Jortner, which is still in use today[REF]. This describes the electron as being solvated by ammonia molecules. The electron polarises the ammonia, which causes a potential well to develop, where the potential is constant within the cavity, and varies outside as in equation 4.3 and 4.4. A 1s to 2p transition in this potential well corresponds to 0.8eV, which matches the peak in the optical absorption, this is thought to be responsible for the blue colour of these solutions (see figure 9).

$$V(r) = \frac{-e^2}{R}(\frac{1}{\epsilon_\infty} - \frac{1}{\epsilon_0}), r < R \tag{4.3}$$

$$V(r) = \frac{-e^2}{r}(\frac{1}{\epsilon_\infty} - \frac{1}{\epsilon_0}), R > r \tag{4.4}$$

Conventional hydrogen bonding is replaced by $H \leftrightsquigarrow H$ bonding as concentration is increased. Note that the electron probability in terms of position is zero at the centre of the cavity, as seen in figure 10[REF].

DFT suggests that 5 ammonia molecules could solvate the electron, although 8 is also stable, forming two smaller cavities with an ammonia molecule in the

Figure 8: A schematic representation of the process of solvation of an electron (ref)

middle, suggesting 5-8 ammonia, molecules solvating the electron is stable[REF].

The dimer is two monomer complexes which have aggregated, they are spin paired as seen by the energetics from DFT. Larger clusters of monomers show that the maximum electron density is between the hydrogens on the solvating ammonias, suggesting that aggregation forms bands and transitions to a metallic state[REF].

The long tail of these solutions is unusual as a 1s to 2p transition should give a symmetrical lineshape. DFT calculations show that this is due to transitions to higher states above 2p, with higher transitions having weaker oscillator strengths and therefore contributing less to the spectrum[REF].

Also note that increasing T red shifts the curve. This corresponds with a decrease in paramagnetic polar susceptibility, suggesting that the formation of diamagnetic species is responsible[REF]. The monomer also exhibits optical

Figure 9: A schematic representation of Jortner model (ref)

absorption in this region, which also has a symmetric line shape but has an energy in the same region, which may contribute to the asymmetry[REF].

4.3.2 Pairing

ESR evidence suggests that the cations are always associated with the electron, and so the ion may be needed to stabilise the electron[REF].

It is thought that spin pairing occurs in the same cavity, with two electrons being trapped in one cavity. Spin paired electrons are lower in energy than unpaired, the diamagnetic state is lower in energy than the triplet or doublet state by several kT, and so we expect that two electrons in a cavity will be spin paired. Evidence for pairing comes from magnetic data. The molar spin susceptibility decreases, suggesting the number of diamagnetic species increases[REF]. At 0.1MPM 90% of the electrons are spin paired.

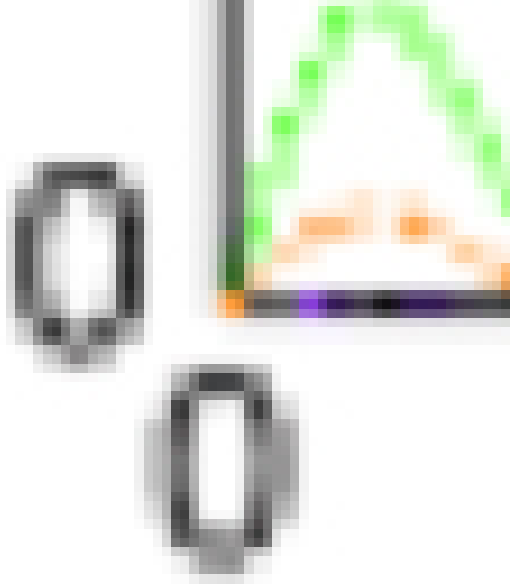

Figure 10: The probability with respect to position of the electron as afunction of distance form the centre of the solvation shell

4.4 Radiolysis

Electrons can be injected into these solutions from an accelerator[REF]. This has been performed through quartz with electrons of energies 4-5MeV. These pulses give approximately $10^8 eV g^{-1}$ to the sample per pulse. The solvated electron in this scenario is thought to be secondary, caused by the ionisation of ammonia via the following reactions:

$$NH_3 + radiation \rightarrow H + NH_3^+ + e^- \tag{4.5}$$

$$NH_3^+ + NH_3 \rightarrow NH_4^+ + NH_2^* \tag{4.6}$$

$$e^- + NH_3 \rightarrow e^-_{(s)} \tag{4.7}$$

$$e^-_{(s)} + NH_4^+ \rightarrow H + NH_3 \tag{4.8}$$

$$e^-_{(s)} + NH_2^* \rightarrow NH_2^- \tag{4.9}$$

$$e^-_{(s)} + e^-_{(s)} \rightarrow H_2 + 2NH_2^- (very slow) \tag{4.10}$$

$$e^-_{(s)} + NH_3 \rightarrow H + NH_2^- \tag{4.11}$$

4.5 Intermediate Regime

All species in figure 2 will be seen in this regime. As metal is added spin pairing increases, and this occurs up to 1MPM, where spin pairing is complete[REF]. Two electrons in a cavity are only stable for many ammonia molecules solvating, and so this becomes less common as concentration is increased. The transition to the metallic state appears to be when the $3a_1$ (LUMOs) orbitals of NH_3 are all partially occupied[REF].

5 Transition and Phase Separation

5.1 Introduction

The transition to the metallic state appears to be intimately linked to the phase separation seen in these solutions. The onset of metallisation depends on the metal (and the solvent for other systems), and a miscibility gap, which is an inaccessible region of the phase diagram (see figures 3, 4, 5) is also present in this region. Here there is phase separation with the denser blue electrolytic solution sitting below the metallic liquid, see figure 11.

The metallic region shows a huge conductivity change across the metallization region, also accompanied by changes in viscosity, surface tension and magnetic properties[ref]. We also see the disappearance of the characteristic blue colour in this region. The metallic state has delocalised Bloch waves, in non-metallic they are localised (Wannier) functions[REF]. The electron crystal (Wigner lattice) is an idea proposed for this transition, but in general isn't helpful.

The reason for the phase separation is still debated, it can be described as a liquid-vapour phase separation within the ammonia matrix, however there are some ideas hinting at a more spectacular reason.

5.2 Models and explanations

Resistivity is suggested to be due to scattering of high velocity delocalised electrons from the solvated metal, and from the dipole moments of the free ammonia molecules[REF]. We therefore see a decrease in resistivity at high concentrations, as the ammonia molecules become scarcer. DFT calculations suggest that the aggregation of monomer units decreases distance between localised electrons (sitting between the N and H atoms on the solvating ammonia molecules), therefore lowering the tunnelling barrier, therefore allowing electrons to become delocalised.

The solution goes through the following regimes during the metal-non-metal transition[REF]:

- A metallic regime where mean free path exceeds inter-atomic spacing (propagation with occasional scattering)

Figure 11: The phase separation boundary. The two liquids are completely immiscible

- Strong scattering, diffusion or Brownian motion with mean free paths roughly equal to order of inter-atomic distances
- Inhomogeneous regime where fluctuations produce macroscopic inhomogeneities and differences in conduction mechanism.
- A Mott-Cohen-Fritzsche-Ovshinsky regime where $N(E_F)$ is not small at Fermi level, states are localised so conduction is primarily via hopping.
- Semiconducting state where no states are at the Fermi level.

The transition can also be thought of in terms of the coulomb screening no longer being able to bind the state as distances are reduced.

Mott believed that the discontinuity in the free carriers at the metallization concentration caused a kink in the free energy curve and thus a phase separation[REF]. The Mott criterion is discussed next.

5.3 Mott criterion

Mott gave an experimental criterion which related the Bohr radius to the critical carrier concentration. It has been shown that this can be modified with an effective Bohr radius, which is for a realistic wave-function, often derived experimentally[REF]. The modified criterion is:

$$n_c^{\frac{1}{3}} a_H^* = 0.26 \pm 0.05 \tag{5.1}$$

Note that the usual Bohr radius (unmodified) is given by[REF]:

$$a_H = \frac{K^2}{m^* e^2} \tag{5.2}$$

Where K is the background dielectric constant, m* is the effective electron mass and a_H^* is the Bohr radius of a realistic wave-function. Note that a realistic wave-function is needed as this criterion assumes spherical potentials, and therefore that the critical carrier density should be independent of the donor atom. This isn't observed but the scaled form fixes this (this is valid over a variation in 600Å[REF]). This criterion gives 3.87 MPM as the critical concentration for Lithium-ammonia solutions.

5.3.1 Hubbard tight binding

The Hubbard tight binding model gives another criterion for metal transition[REF]:

$$\frac{W}{U} \approx 1 \tag{5.3}$$

where W is the unperturbed bandwidth of an array of one electron states, and U is the intra-donor coulomb repulsion energy.

If we assume that the intra-donor coulomb repulsion energy is the primary driver of the transition, we can thus predict the onset of the transition.

For the conduction band, the use of an isotropic wave-function is appropriate[REF]:

$$\psi(r)_{EM} = \sum_{j=1}^{N} \alpha_j F_j(r) \phi_j(r) \tag{5.4}$$

where N is the number of conduction band minima in k space, alpha are numerical coefficients and ψ is a Bloch wave at the j^{th} minima. F represents hydrogenic envelope functions.

Note that this gives simple hydrogen arguments for bandwidth and repulsions for s like state only, and also that although W and U are dependent on the host dielectric, the Hubbard ratio is not. Therefore the transition reduces to a one electron problem, with the potential and kinetic energy terms competing.

The Hubbard model gives the right hand side of the Mott criterion as 0.26[REF].

5.3.2 Pitzer model

Pitzer suggested that ammonia acts as a host matrix, and the phase separation is due to the 'gaseous' dilute metal and the 'liquid' concentrated metal phases within the ammonia[REF].

When semiconductors are 'matrix-bound' Mott's criterion is shifted due to the deformed electron cloud giving a larger Bohr radius. Thus a lower density is needed for metallization, and therefore a lower critical density is obtained.

The host dielectric properties are reduced in energies by a factor of K^{-2}, and all distances increase by a factor of K[REF]. For Methyl-amine solutions, differences in the transition concentration are observed. It has been shown by Edwards that the effective dielectric constant shifts, and this is due to a higher degree of spatial confinement of the electron, therefore successfully explaining differences between similar systems.

5.3.3 Ogg's model

Ogg suggested that the miscibility gap was due to an unfavourable free energy change[REF]. He believed that the bi-polarons (paired electrons linked to a matrix deformation) acted as Bosons, and as such obeyed Bose-Einstein statistics (as they have S=0). He concluded that spin paired electrons must be mobile due to high conductivity in electrolytic solutions and transference data suggesting the mobilities were primarily influenced by negative carriers.

Therefore we would expect a condensation at[REF]:

$$T_C = \frac{3.31h^2n^{\frac{2}{3}}}{m^*k_B} = 2.2910^{-11}\frac{m_e}{m*}n^{\frac{2}{3}}K \tag{5.5}$$

For sodium solutions, the upper consolute point is at 4.2MPM. This gives a number of trapped paired electrons, then using $m^* = 2m_e$ gives T_c= 900K. This temperature may be depressed due to an effective mass of the bi-polarons not equal to $2m_e$, or due to incomplete pairing of electrons. This condensation is what Ogg thought was responsible for the miscibility gap.

6 Solid and Glassy Compounds and Possible Superconductivity

6.1 History

As already mentioned, Ogg proposed the idea of the miscibility gap being due to an unfavourable free energy change upon Bose-Einstein condensation, causing the phase separation seen. He came to this conclusion following a series of experiments in which he attempted to quench metal-ammonia solutions in order to form a glass. He believed this would allow access to the miscibility gap, where a Bose-Einstein condensate might exist. It is noteworthy that the ideas he proposed to explain superconductivity in terms of paired electrons (1946) was well before BCS theory (1957)[REF], although current theory (including BCS) would not successfully explain an amorphous superconductor.

6.2 Ogg

The experimental details and key findings of Oggs experiments are presented below[REF]:

- Sodium-ammonia solutions were used in these tests. These were quenched into liquid air from $-33°C$ in several different vessels
- He claimed that he saw solids which retained their blue colour, and concentration solutions had a bronze lustre
- Ogg noted that dilute solutions of approximately 1MPM phase separated into two dilute phases upon rapid freezing
- Upon quenching he noted a huge increase in conductivity when measuring with platinum electrodes. He noted that residual resistivity was probably due to cracked electrodes as this occurred frequently and prevented many measurements being recorded
- He also tested superconductivity using an annular glass ring, this was plunged into liquid air between strong magnets, and then persistent currents were later measured with a magnetometer
- In over 200 trials, only 7 worked. Ogg suggested the formation of micromosaics within the solid, where relatively slow cooling had prevented an homogeneous glassy state

Initial data in Studsvik (figure 12) suggests that these glasses can be formed, however repeatability has been an issue in a recent ISIS experiment[REF]. This was a similar problem for Ogg, and this problem has been ignored for many years due to lack of reproducibility. Initial data suggests that the glass is less dense than the liquid. Initial SQUID data (figure 13) suggests that fast quenching gives a different response when increasing the field compared to slow cooled under different B fields and the liquid state.

6.3 Solids

Below the eutectic a hexagonal phase exists in these solutions, see figure 14 [REF].

Figure 12: Initial neutron scattering data from Studvik for liquid and quenched Li-NH_3

Figure 13: Initial SQUID data for quenched $LI - NH_3$ solutions

Figure 14: The solid phase structure of $Li - NH_3$

7 Other Solvents

7.1 Introduction

Electrons can be trapped in other solvents, although typically the lifetimes are much shorter. Table 7.1 shows species which solvate electrons, the energy of the solvated electron absorption peak and the metal anion species, if any, dissolved for this measurement[REF]. Note that we expect in general there to be no dependence on anion, but a small dependence is usually seen.

Name	$\hbar\omega_{max}$ (eV)	Metal anion
Glycerol	2.35	-
Ethylene glycol	2.16	-
Methanol	1.97	-
Ethanol	1.77	-
Water	1.72	-
Isopropanol	1.51	-
Methylamine	0.95	Na^-
Ethylenediamine	0.94	Na^-
Ammonia	0.80	-
Ethylamine	0.69	Na^-
Diethylamine	0.65	Na^-
Bis(2-methoxy-ethyl)ether	0.65	Na^-
Diethyl ether	0.64	Na^-
Dimethoxyethane	0.60	Na^-
Tetrahydrofuran	0.58	Na^-
Methyletra-hydrofuran	0.57	-
Hexamethylphosphorictramide	0.55	Na^-

Table 1: The species which solvate electrons, the energy of the solvated electron absorption peak and the metal anion species, if any, dissolved for this measurement

7.2 Other Amines

Other amines tend to work, e.g. methyl-amine[REF]. The phase diagram for Li-Methylamine is shown in figure 15.

Figure 15: The Li-Methylamine phase diagram

7.3 H_2O

The solvated electron is also seen in H_2O, recent work shows the blue colour in a coulomb explosion. Figure 16 shows a blue colour observed before a coulomb explosion for NaK dropped into water[REF].

Figure 16: An image of the blue colour, indicative of a trapped electron, prior to a coulomb explosion due to NaK in H_2O